

# DocPedia: Unleashing the Power of Large Multimodal Model in the Frequency Domain for Versatile Document Understanding

Hao Feng<sup>1,2,♣,\*</sup> Qi Liu<sup>2,\*</sup>, Hao Liu<sup>2,\*</sup>,<sup>‡</sup> Wengang Zhou<sup>1,‡</sup> Houqiang Li<sup>1</sup> Can Huang<sup>2,‡</sup>

<sup>1</sup> University of Science and Technology of China, <sup>2</sup> ByteDance Inc.,  
 {haof}@mail.ustc.edu.cn, {zhwg, lihq}@ustc.edu.cn,  
 {liuqi.nero, haoliu.0128, can.huang}@bytedance.com

## Abstract

This work presents DocPedia, a novel large multimodal model (LMM) for versatile OCR-free document understanding, capable of parsing images up to  $2,560 \times 2,560$  resolution. Unlike existing work either struggle with high-resolution documents or give up the large language model thus vision or language ability constrained, our DocPedia directly processes visual input in the frequency domain rather than the pixel space. The unique characteristic enables DocPedia to capture a greater amount of visual and textual information using a limited number of visual tokens. To consistently enhance both perception and comprehension abilities of our model, we develop a dual-stage training strategy and enrich instructions/annotations of all training tasks covering multiple document types. Extensive quantitative and qualitative experiments conducted on various publicly available benchmarks confirm the mutual benefits of jointly learning perception and comprehension tasks. The results provide further evidence of the effectiveness and superior performance of our DocPedia over other methods.

## 1. Introduction

Document understanding [42] is a critical and challenging task that sits at the intersection of computer vision and natural language processing. It involves the *perception* and *comprehension* in terms of visual and textual content embedded within document images. The difficulty of this task stems from the diverse and complex formats of high-resolution documents, where the sparse or dense texts are intertwined with graphics and tables. The accurate parsing of documents not only propels the digitization of archival materials but also facilitates the document automation in current data-rich world, such as information extraction [15, 18, 30] and visual question answering [9, 31, 52, 53].

\*Equal contribution. ♣ Interns at ByteDance. ‡ Project lead.

†Corresponding authors: Wengang Zhou and Can Huang.

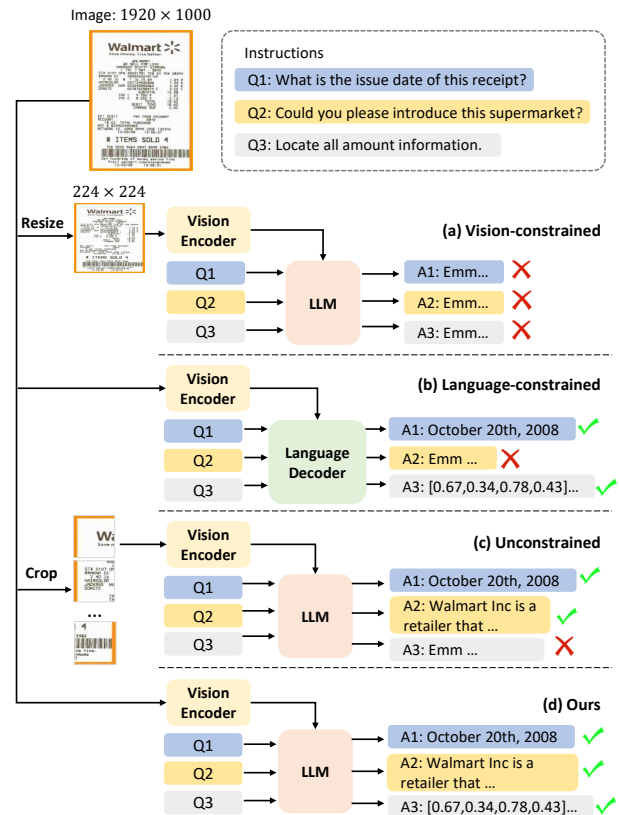


Figure 1. Comparisons of existing pipelines for document understanding. Contrasting with (a) vision-constrained, (b) language-constrained, and (c) unconstrained methods, our DocPedia efficiently processes high-resolution document images and performs logical reasoning using the world knowledge of large language models. The instructions Q1, Q2, and Q3 evaluate the text recognition, world knowledge, and text localization abilities, respectively.

Many early attempts [2, 3, 11, 13, 21, 36, 43, 49, 50] in the field follow a perceive-then-comprehend paradigm, initially involving Optical Character Recognition (OCR) [22, 39] of document images, followed by the fusion of textual, layout, and visual features for content parsing. However,

the individual processing step of OCR may precipitate the accumulation of errors. Furthermore, considering the intrinsic interweaving of visual elements and textual segments within documents, the reciprocity between perception and comprehension awaits further exploration.

To attack the issue, OCR-free solutions have emerged as recent prevailing approaches in the field. Among them, most models commonly generate a sequence of tokens that can be converted into a target string [9, 51–53, 55] or a structured format data [18, 20, 31]. Such generative models are skilled at synthesizing and rephrasing information, which naturally can unveil the implicit content or purpose behind the source material, as well as provide deeper insights and more versatile responses to inquiries. As depicted in Fig. 1, they can be mainly categorized into three groups, namely (a) *vision-constrained*, (b) *language-constrained*, and (c) *unconstrained* types, described next.

Specifically, in vision-constrained methodologies such as LLaVAR [55], mPLUG-DocOwl [51], and UniDoc [9], the visual encoders largely rely on a pre-trained CLIP-ViT [38], operating at input resolutions of 224 or 336. These resolutions are designed for images featuring texts in medium or large font sizes, *e.g.*, scene text, but prove inadequate for text-intensive high-resolution documents where more details are indispensable [27]. As shown in Fig. 1 (a), when a high-resolution supermarket receipt is downsampled to 224 for model input, the text becomes unreadable, rendering these methods incapable of answering the three presented instructions. In contrast, language-constrained approaches, including Donut [18], KOSMOS-2.5 [31], and Pix2Struct [20], employ high-resolution input for training their models with a vision encoder. They abandon the use of large language models (LLMs) in vision-constrained methods [9, 51, 55], and instead opt for a lightweight language decoder [46]. While these approaches demonstrate promising perception ability, their comprehension performance is often compromised. This is because the vital components of robust logical reasoning and extensive world knowledge, typically provided by the LLM, are not adequately incorporated. Taking Fig. 1 (b) for example, in response to the instruction Q2, these models falter in providing accurate answers due to a deficiency in pertinent knowledge.

The *status quo* triggers a question: *Is there a feasible approach to maintain both perception and comprehension abilities without compromising vision and language?*

To mitigate the problem in above both categories, unconstrained method [52] (Fig. 1 (c)) takes a further step by proposing a shape-adaptive cropping strategy. This strategy involves cropping high-resolution images into patches, which are then used in conjunction with a frozen low-resolution CLIP-ViT [38] and LLM. However, this heuristic-based crop strategy may lead to semantic discontinuities, even after fusion is performed. Furthermore, the

features extracted by CLIP-ViT [38] are not well-suited for tasks that require fine-grained local detail, such as text detection [9] or grounding (refer to Q3 in Fig. 1 (c)).

To answer the question aforementioned, this work re-inspects the problem through the lens of frequency and proposes DocPedia, a novel yet effective Large Multimodal Model (LMM), aiming to achieve versatile OCR-free document understanding. DocPedia is capable of parsing high-resolution document images up to  $2,560 \times 2,560$ , and harnessing the extensive world knowledge and powerful inference capabilities offered by LLMs [7, 45]. This integration aims to enhance both perception and comprehension aspects. Technically, contrasting with previous LMMs in the field, DocPedia directly processes visual input in the frequency domain [1, 23, 24, 47] rather than the pixel space. This unique characteristic of the frequency domain enables DocPedia to capture a greater amount of visual and textual information using a limited number of visual tokens.

Employing this effective architecture, we train our DocPedia with two phases: i) *text-aware pre-training* and ii) *context-aware fine-tuning*. During the pre-training stage, the vision encoder is trained to align the frequency domain features with a LLM [7], incorporating various perception tasks across both document and natural scene contexts, such as text detection [22], spotting [26], paragraph reading, image captioning [12], and *etc.* In the subsequent fine-tuning stage, the focus shifts to the simultaneous learning of perception and comprehension, *e.g.*, lower-level reading-related tasks and higher-level document understanding. To ensure the robustness of the model as well as a consistent response style, we enrich the instructions and annotations of all these tasks with GPT [6]. Extensive quantitative and qualitative experiments are performed on this constructed large-scale instruction tuning dataset covering multiple document types. The results demonstrate the mutual benefits of jointly learning perception and comprehension tasks.

The contributions are summarized as follows:

- To the best of our knowledge, we are the first to scale a large multimodal model for document understanding tasks to the resolution of  $2,560 \times 2,560$ .
- We innovatively transform image domain inputs into frequency ones, enabling capturing more visual and textual information using a limited number of visual tokens.
- We achieved superior performance on multiple publicly available benchmark datasets and conducted extensive experiments to validate the effectiveness of DocPedia.

## 2. Related Work

In the following, we provide an overview of existing research in the field of document understanding. This body of work is categorized into two distinct types: OCR-driven and OCR-free methodologies, discussed next.

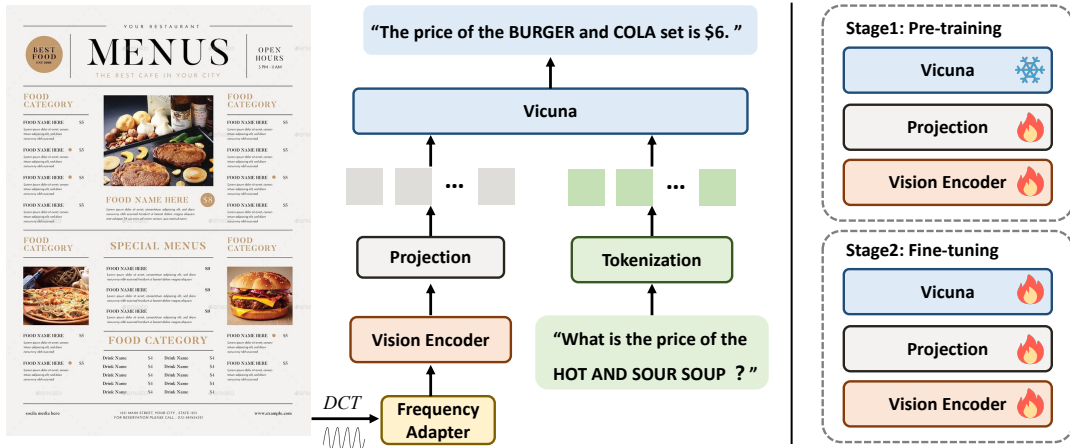


Figure 2. An overview of the DocPedia. Given a document image, DocPedia initially applies JPEG DCT extraction to retrieve the DCT coefficients, which are then processed by a frequency adapter before feeding into a vision encoder. The resultant tokens are combined with instruction-derived tokens, and fed into a large language model (LLM). Then, based on these textual and visual information within the document as well as the intent of instruction, the LLM leverages its rich world knowledge to generate a logically coherent response.

## 2.1. OCR-driven Document Understanding

This section outlines methods that initiate with text extraction from document images, followed by the integration of textual, layout, and visual features for thorough content analysis. Prominent among these are the LayoutLM series [13, 49, 50], which enhance text and layout modeling and integrate complex multimodal pre-training for richer representation learning. Wukong-Reader [3] employs pre-training objectives to exploit the structural knowledge of document textlines, incorporating textline-region contrastive learning for advanced visual document understanding. StrucText [21] combines a segment-token aligned encoder with diverse pre-training tasks, targeting enhanced structured text analysis in visually rich documents. DocFormer [2] fuses text, vision, and spatial information using a distinct transformer architecture. However, the dependence of these methods on Optical Character Recognition (OCR) can result in error accumulation, raising efficacy concerns regarding the segregation of OCR in the context of the intertwined nature of visual and textual elements in documents.

## 2.2. OCR-free Document Understanding

To address this issue, prevailing OCR-free models excel in generating token sequences for varied responses and structured information synthesis, thereby offering enhanced insights and versatility in content creation and inquiry response. Typically, LLaVAR [55] enhances document understanding by improving interaction skills with humans and boosting performance on text-rich image tasks, building upon its predecessor LLaVA [25] with advanced visual instruction tuning techniques. Based on the large multimodal model mPLUG-Owl [53], mPLUG-DocOwl [51] integrates a unified instruction tuning strategy across di-

verse document data. UniDoc [9] combines foundational OCR learning with text-rich image comprehension tasks, markedly boosting text scene image understanding. Despite their strong representational skills and world knowledge from extensively pre-trained CLIP-ViT [38] and large language models, these methods are limited to processing images with larger, sparser text due to the pre-trained visual models' lower resolution constraints. StrucTextv2 [54] employs self-supervised pre-training for document images, adeptly integrating masked image and language modeling [8, 10] to enhance performance. Donut [18] introduces an end-to-end trainable model that overcomes OCR limitations by using a synthetic document image generator for pre-training, enhancing performance in document understanding tasks. Pix2Struct [20] through its unique pretraining on web page screenshots parsed into HTML, introduces a variable-resolution input and integrated language-vision approach. As an evolution of Kosmos-2 [37], Kosmos-2.5 [31] processes text-rich images, skillfully blending spatial text block creation and structured markdown generation in a streamlined, decoder-only model. UReader [52] innovatively employs a shape-adaptive cropping module for high-resolution image processing.

While these work exhibit outstanding outcomes in various aspects, they either struggle with handling high-resolution input or face challenges due to a lack of world knowledge. This underscores the future research endeavors: the development of an intelligent system adept at handling documents of various types and resolutions.

## 3. Method

Fig. 2 presents an overview of DocPedia. It consists of two training phases: (a) text-aware pre-training to align the vi-

sual features from the frequency domain to the large language model, and (b) context-aware fine-tuning for learning the parsing of documents. In the following, we first delineate the network architecture of DocPedia, followed by a detailed exposition of its two training phases.

### 3.1. Architecture of DocPedia

Given an input RGB document image, we first resize it to our designated training scale of  $H \times W$  to obtain the image  $I$ . By default, both  $H$  and  $W$  are set as 2,560. Here we preserve the aspect ratio during the resizing process to prevent distortion of textual elements. Then, as shown in Fig. 3, we apply the JPEG DCT extraction [1, 47] to retrieve the DCT coefficients for the  $Y$ ,  $Cb$ , and  $Cr$  channels. The DCT coefficients are scaled down due to  $8 \times 8$  block processing for the luminance component ( $Y$ ) and additional chroma subsampling for color components ( $Cb$  and  $Cr$ ), resulting in  $\frac{1}{8}$  and  $\frac{1}{16}$  scales respectively. Each of them features  $C$  channels. After that, we upscale  $Cb$  and  $Cr$  to a  $\frac{1}{8}$  scale based on bilinear interpolation, followed by a concatenation along the channel dimension. Subsequent to this is a  $1 \times 1$  convolutional layer, employed to map the channel dimension of the concatenated map to that of the following backbone’s input. Through these operations, we acquire the frequency domain counterpart of image  $I$ , denoted as  $F$ .

Next, we feed  $F$  into the Swin Transformer [28], a visual backbone that leverages shifted windowing schemes to efficiently model spatial hierarchies. In our implementation, we remove the 1/4 scale downsampling module originally present before stage 1. The output of the visual backbone is a feature map downsampled by a factor of 1/64. It is subsequently flattened, resulting in  $\frac{H}{64} \times \frac{W}{64}$  tokens, each with a dimensionality of 1,024. Drawing inspiration from the paradigms of advanced large multimodal models [25, 56], we employ a linear layer to align these tokens with the input token dimension of the following large language model [7]. Finally, the dimensionally aligned visual tokens are concatenated with the tokens transformed from the language instructions. This concatenated sequence is then fed into the LLM, generating the output response.

### 3.2. Text-aware Pre-training

To develop a vision encoder capable of processing frequency domain representation input and align it with the feature space of the following large language model [7], we first undertook extensive text-aware pre-training. During this stage, we freeze the large language model, focusing on the optimization of the vision encoder and its subsequent linear projector, as illustrated in Fig. 2.

Specifically, our pre-training encompassed a variety of perception tasks, including text detection [22], recognition [48], spotting [26], paragraph reading, full-text reading [18], and image captioning [12]. The first three tasks

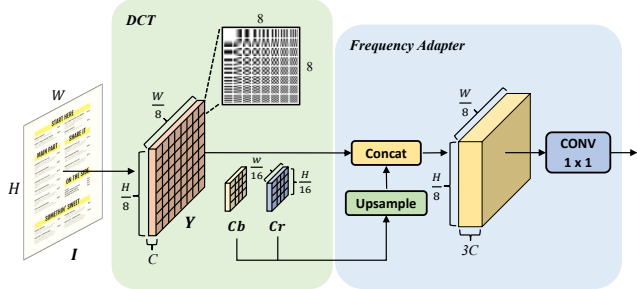


Figure 3. Schematic illustration of the DCT transformation and frequency adapter module in DocPedia.

are foundational OCR tasks. “Paragraph reading” denotes the reading of the text within a specified bounding box (see bottom case in Fig. 4), whereas “full-text reading” refers to deciphering all text in the image. It is worth noting that the first five tasks focus on a diverse array of document images, while the final task targets natural scene images. This comprehensive pre-training enables the vision encoder of our DocPedia to effectively perceive textual and visual information from both document and natural scene images.

### 3.3. Context-aware Fine-tuning

In the fine-tuning phase, we concurrently cultivate the perception and comprehension capabilities of DocPedia. Concretely, within each batch of training data, one half is dedicated to the five types of OCR tasks outlined in the pre-training phase, while the other half comprises tasks that demand a higher level of semantic understanding related to document [33] and scene [25]. We argue that the concurrent learning of lower-level perceptual abilities and the cultivation of higher-level understanding capabilities can maximize the performance of the model. During this stage, we unfreeze the LLM and fine-tune the entire model.

Stage	Image	Instruction	Task	# Conv
Pre-training	Scene	LLaVA [25]	$\mathcal{C}$	595K
	PDF	OCR	$\mathcal{D}, \mathcal{R}, \mathcal{S}, \mathcal{R}_p, \mathcal{R}_f$	325K
	PPT	OCR	$\mathcal{D}, \mathcal{R}, \mathcal{S}, \mathcal{R}_p, \mathcal{R}_f$	600K
Fine-tuning	PDF	OCR	$\mathcal{D}, \mathcal{R}, \mathcal{S}, \mathcal{R}_p, \mathcal{R}_f$	325K
	PPT	OCR	$\mathcal{D}, \mathcal{R}, \mathcal{S}, \mathcal{R}_p, \mathcal{R}_f$	600K
	Scene	LLaVA [25]	$\mathcal{U}$	158K
	Benchmark	GPT	$\mathcal{U}$	370K

Table 1. Summary of the training data statistics across two stages. The symbols represent various instruction-following tasks as follows:  $\mathcal{D}$  for text detection,  $\mathcal{R}$  for text recognition,  $\mathcal{S}$  for text spotting,  $\mathcal{R}_p$  for paragraph reading,  $\mathcal{R}_f$  for full-text reading,  $\mathcal{C}$  for image captioning, and  $\mathcal{U}$  for document understanding.

Method	Resolution	KIE			VQA						Avg.
		FUNSD	SROIE	POIE	DocVQA	ChartQA	STVQA	OCRVQA	TextVQA	InfoVQA	
BLIP-2 OPT <sub>6.7b</sub>	224	0.00	0.00	0.02	0.82	7.44	13.36	10.58	21.18	8.82	6.91
BLIP-2 FlanT5 <sub>XXL</sub>	224	1.19	0.20	2.52	4.86	7.20	21.70	30.74	32.18	10.17	12.31
OpenFlamingo	224	0.85	0.12	2.12	5.05	9.12	19.32	27.82	29.08	14.99	12.05
LLaVA	224	1.02	0.12	2.09	4.49	7.28	22.08	11.36	28.86	13.78	10.12
MiniGPT-4	224	1.19	0.04	1.31	2.97	4.32	14.02	11.52	18.72	13.32	7.49
mPLUG-Owl	224	1.02	0.64	3.26	6.88	9.52	29.26	28.62	40.28	<b>16.46</b>	15.10
LLaVAR	224	1.02	1.36	6.48	6.73	8.00	30.36	29.38	39.40	12.25	15.00
UniDoc	224	1.19	1.40	3.92	6.47	10.48	30.78	34.50	40.72	13.75	15.91
<b>DocPedia</b>	1920	<b>18.75</b>	<b>17.01</b>	<b>32.17</b>	<b>37.83</b>	<b>40.13</b>	<b>41.06</b>	<b>40.80</b>	<b>53.35</b>	12.71	<b>32.65</b>
<b>DocPedia<sup>†</sup></b>	2560	<b>29.86</b>	<b>21.44</b>	<b>39.94</b>	<b>47.08</b>	<b>46.88</b>	<b>45.54</b>	<b>57.20</b>	<b>60.18</b>	<b>15.21</b>	<b>40.37</b>
Supervised-SOTA	/	<b>93.12</b>	<b>98.70</b>	<b>79.54</b>	<b>90.16</b>	<b>70.50</b>	<b>69.60</b>	<b>68.10</b>	<b>73.67</b>	<b>36.82</b>	<b>75.58</b>

Table 2. Quantitative accuracy (%) comparison with existing large multimodal models (LMMs) on key information extraction (KIE) and visual question answering (VQA) benchmarks. “Supervised-SOTA” reported in [27] denotes specialized models that have been fine-tuned on the training set of the corresponding benchmark. Red highlights indicate the highest achieved results and blue signifies second-best.

Type	Example
Detection	“Where are the texts located in the photo?”
Recognition	“Recognize all the text in this image.”
Spotting	“Identify all the text in the shot return their coordinates in the format of [x1,y1,x2,y2].”
Paragraph Reading	“Tell me about the content in the area marked as [0.124,0.276,0.353,0.487] of the frame.”
Full Text Reading	“Convey the entire content of this pic to me.”

Table 3. Different types of OCR instructions and their examples.

## 4. Dataset Construction

To train our DocPedia, we construct a large-scale multimodal instruction following dataset. The statistical data employed during the pre-training and fine-tuning phases are summarized in Table 1. We detail them in the following.

### 4.1. Pre-training

During the pre-training phase, our focus was on the learning of perceptual abilities, particularly in the context of text perception. As illustrated in Table 1, we amassed a dataset comprising 600,000 PowerPoint (PPT) images and 325,000 PDF images. The PowerPoint images are sourced from the “Common Crawl” dataset<sup>1</sup>, an extensive web corpus encompassing publicly accessible web pages. The PDF images are sourced from arXiv<sup>2</sup>, an established online platform for scientists to publish pre-print research papers.

For each of these images, we randomly selected an Optical Character Recognition (OCR) task type as described in Sec. 3.2 and then constructed corresponding instructions and responses [9]. On one hand, to ensure instruction diversity, we generated multiple variations of instructions for each OCR task using GPT-3.5 [6]. In Table 3, we present one exemplar for each of the five text-aware perceptual

<sup>1</sup><https://commoncrawl.org/>

<sup>2</sup><https://arxiv.org/>

tasks. For further examples, please refer to the supplementary materials. On the other hand, for their responses, we employed a standardized format (see Fig. 4). In addition to the aforementioned data, we enriched our dataset with 595,000 caption entries from LLaVA [25], aiming to enhance the DocPedia’s perceptual abilities in natural scenes.

### 4.2. Fine-tuning

Furthermore, during the fine-tuning phase, we first employed the same data utilized during the pre-training phase, comprising 325,000 PDF and 600,000 PPT images. Building upon this, we introduced an extra 370,000 entries from seven visual question answering benchmark datasets, including DocVQA [33], OCRVQA [35], TextVQA [40], InfoVQA [34], ChartVQA [32], FigureVQA [17], and PlotVQA. Notably, as the responses in these datasets are typically concise, containing only the answer itself, we employed GPT-3.5 [6] to expand these responses into complete sentences. This adaptation was done to align with the characteristic comprehensive and detailed response style of large language models [7]. Besides, we supplemented the training data with 158,000 instruction tuning data for natural scene understanding from LLaVA [25]. Our experiments demonstrate the effectiveness of a fine-tuning strategy that concurrently learns perceptual and understanding abilities.

## 5. Experiment

### 5.1. Implementation Details

To implement DocPedia, we adopted a one-cycle learning rate strategy [41]. For the pre-training phase, the peak learning rate was established at 1e-3, which was set as 1e-5 during the subsequent fine-tuning phase. We maintained batch sizes of 64 and 8 for the pre-training and fine-tuning stages, respectively. We employ the AdamW optimizer [29] and both training stages were performed on eight A100 GPUs, each spanning just a single epoch.

For performance assessment, a temperature parameter of

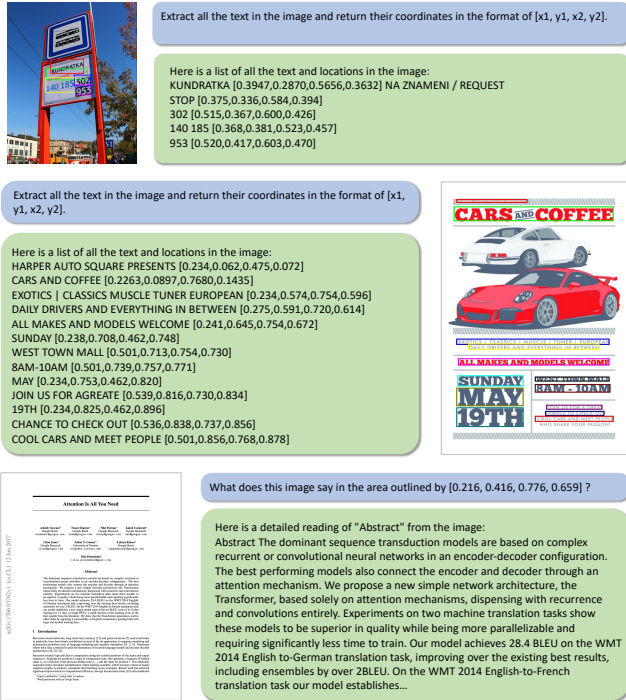


Figure 4. Exemplary demonstrations of DocPedia’s advanced text perception capabilities. The three instances illustrate its adeptness in accurately identifying and localizing text in scene and document images, and demonstrating proficient paragraph reading skills. We visualized the bounding boxes within the responses in the images. For the last case, subsequent text readouts have been omitted for display convenience. Zoom in for best view.

0.2 was utilized in both quantitative and qualitative evaluations. We adopted the accuracy metric, where a response generated by the model is considered correct if it contains the string present in the ground truth [27].

## 5.2. Results

We further conducted both quantitative and qualitative evaluations of the current state-of-the-art multimodal large-scale models in comparison to our proposed method.

**Qualitative results.** We qualitatively evaluate DocPedia’s perception and comprehension capabilities on high-resolution scene text and document images. Firstly, in terms of the perception capabilities, as illustrated in Fig. 4, our DocPedia can accurately locate and identify text in both scenes and high-resolution documents, which is attributed to the training of fundamental OCR tasks in Table 1. Secondly, regarding comprehension abilities, as demonstrated in Fig. 5, the examples in the first two rows indicate that DocPedia can perceive and understand the visual and textual information in images to provide accurate responses, based on the intention of the instructions. Moreover, the examples in the bottom row illustrate that DocPedia is capable

of integrating the content of instructions, visual and textual information within images, and its large language model’s rich world knowledge to formulate responses. These results demonstrate DocPedia’s robust multimodal comprehension capabilities. For additional examples, please refer to the supplementary materials.

**Quantitative results.** Furthermore, we conduct a quantitative evaluation of existing large multimodal models and our DocPedia. The results are summarized in Table 2. The benchmarks used for this assessment consist of 3 Key Information Extraction (KIE) datasets, including FUNSD [16], SROIE [14] as well as POIE [19], and 6 Visual Question Answering (VQA) datasets, including DocVQA [33], ChartVQA [32], STVQA [5], OCRVQA [35], TextVQA [40], and InfoVQA [34].

As we can see, on several high-resolution document image benchmarks [14, 16, 19, 32, 33], where the text is dense and tiny, our DocPedia demonstrates significant performance improvements over existing state-of-the-art multimodal large models. Notably, compared to the state-of-the-art LMMs, DocPedia achieved an increase in accuracy by 40.20% on DocVQA [33] and 28.67% on FUNSD [16], respectively. These results underscore the distinct advantages of our approach. Moreover, our method also achieved considerable improvements on high-resolution scene text benchmarks [5, 34, 35, 40], though the enhancements were less pronounced. This can be attributed to two primary factors: firstly, our pre-trained vision encoder was not exposed to large-scale natural scene data as extensively as pre-trained Vision Transformer (ViT) [38] employed in previous LMMs [9, 25, 56]; secondly, in such images, the text often appears more sparsely and is generally larger compared to the dense and tiny textual content in document images.

## 5.3. Ablation Studies

We further conduct ablation studies to validate the efficacy of core settings and components in DocPedia. Note that all experiments were conducted on two benchmark datasets: DocVQA [33] and TextVQA [40]. DocVQA [33] is centered around document comprehension, whereas TextVQA [40] focuses on scene text image understanding. Both datasets are notable for their substantial sample sizes, comprising 5,000 and 5,349 test samples, respectively.

**Impact of training in the frequency domain.** One of the significant contributions of our DocPedia lies in utilizing the frequency domain representation of images as the input for the vision encoder. In Table 4, we evaluate our method’s performance using image inputs and frequency domain inputs on varying scales. For image inputs, three resolution settings were evaluated: 640, 960, and 1,280. Given that the backbone Swin [28] downsamples input by a factor of 32, the resultant token counts are 400, 900, and 1,600, respectively. In experiments with our frequency do-



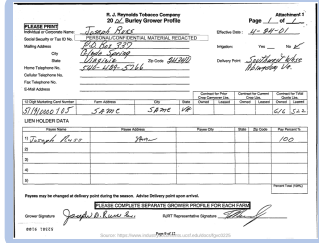
What is the plate number of this truck?

The plate number of this truck is SL 296RN.



What is the processor configuration of the 13-inch MacBook Pro according to the image?

The 13-inch MacBook Pro has a dual-core Intel processor with a clock speed of up to 2.9GHz.



Who is the Grower?

The grower's name is Joseph D. Russell Jr.



What is the price of the BURGER and COLA set?

The price of the BURGER and COLA set is \$15.99.



Who got the most three points before turning 30?

The player who got the most three points before turning 30 is Steph Curry.



Who ordered the items?

The person who ordered the items is Jack Lee.



Please introduce the movie in the image.

Here is a brief introduction of the movie: "Return of the Jedi" is a Star Wars spin-off prequel film that focuses on the young adult character named Rey as she embarks on her journey to find Luke Skywalker while facing off against the evil Kylo Ren and his father, Han Solo.



What is the story of the pokemon in the center of screenshot.

The Pokémon in the center of the screenshot is named Pikachu. It was first introduced as a character in the Pokémon franchise in 1996, and has since become one of the most popular and recognizable characters in the series. Pikachu is known for its lightning-fast speed and ability to electrocute opponents with its tail or back feet. In addition to being featured prominently in numerous games, including the mainline series of Pokémon games and various spin-offs, Pikachu also appears in several animated television shows and movies based on the Pokémon franchise.



Please give the detailed introduction of the second place shown in the image.

Rome is the capital city of Italy and is well-known for its historical and cultural heritage. It was founded on July 21st, 753 BC by Romulus and has since become one of the most influential cities in history. Home to the Colosseum, the iconic amphitheater where gladiators fought in ancient Roman times, as well as numerous other historic sites such as the Forum, Trevi Fountain, and Vatican City, Rome attracts millions of tourists each year who come to explore and admire its architectural marvels and rich history.

Figure 5. Exemplary demonstrations of DocPedia’s image comprehension capabilities. The first two rows primarily showcase DocPedia’s accurate responses to the instructions based on visual and textual information within images. Building on this, the bottom row further exhibits DocPedia’s ability to leverage its extensive world knowledge from its large language model component for responding. The evaluated images include high-resolution textual scene images and document images. Best viewed in color and zoom in.

Method			VQA	
Input	Resolution	Tokens	DocVQA [33]	TextVQA [40]
RGB	640×640	400	13.78	27.56
RGB	960×960	900	21.15	41.18
RGB	1280×1280	1600	29.54	48.80
DCT	1280×1280	400	21.09	45.05
DCT	1920×1920	900	37.83	53.35
DCT	2560×2560	1600	<b>47.08</b>	<b>60.18</b>

Table 4. Ablation experiments regarding the use of various resolutions in the RGB domain and frequency domain as inputs for the vision encoder in DocPedia. “Tokens” refers to the number of tokens outputted by the vision encoder.

Pre-training	Fine-tuning		VQA	
	Perception	Understanding	DocVQA [33]	TextVQA [40]
	✓	✓	21.59	34.17
✓		✓	27.13	48.47
✓	✓	✓	<b>37.83</b>	<b>53.35</b>

Table 5. Ablation experiments concerning the training strategies of DocPedia during the pre-training and fine-tuning phases. All ablations are conducted at a resolution of 1,920×1,920.

main inputs, we tested image resolutions of 1,280, 1,920, and 2,560 for the DCT, resulting in token counts corresponding to the three image-based experimental settings.

As we can see, with the same number of visual tokens, our DocPedia yields better performance. This is attributed to the increased resolution enabling enhanced perception of texture content within images. In experiments where the input resolution is constant (1,280 in Table 4), we observe a slightly enhanced performance with image inputs compared to frequency ones. Note that the number of visual tokens for the latter is only a quarter of that used for the former. This is likely because our frequency-based approach retains a limited number of tokens, leading to some information loss. However, this constraint simultaneously facilitates the incorporation of higher-resolution inputs, up to 2,560×2,560.

In Fig. 6, we further compare the responses of DocPedia to the same academic image and instruction under varying input resolutions. It is observed that the response becomes accurate when the input resolution reaches 2,560.

**Impact of the training strategy.** We further study the impact of our training strategies. Initially, we omitted the pre-training phase, opting instead for a random initialization of the vision encoder. In Table 5, significant performance degradation was observed in the absence of pre-training, underscoring the critical role of feature alignment between the vision encoder and subsequent LLM [7].

Additionally, we examined the fine-tuning strategies. Under default settings, we concurrently learn perceptual

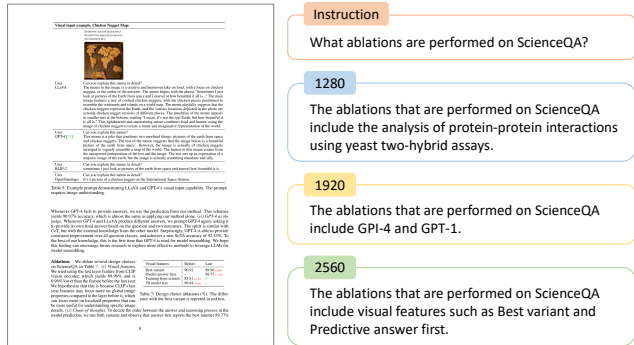


Figure 6. Comparison of DocPedia’s responses to varying resolutions of DCT inputs for the same high-resolution document image, encompassing scales of 1,280, 1,920, and 2,560. The response becomes accurate at the scale of 2,560. Zoom in for best view.

and understanding capabilities, incorporating tasks OCR, image captioning, document understanding, and scene comprehension. Subsequently, we eliminated the OCR and image captioning from the fine-tuning. The results clearly indicated a notable decline in performance, affirming the efficacy of our joint training strategy. This implies that the simultaneous development of foundational perceptual skills augments the acquisition of comprehension abilities.

## 5.4. Limitation Discussion

Furthermore, we discuss the limitations of our DocPedia. Firstly, as illustrated in Table 2, we observe minimal performance improvements on the InforVQA dataset [34]. This highlights one of the constraints of DocPedia. Many images in InforVQA [34] possess extremely high aspect ratios, akin to vertically concatenating multiple pages of images, with some even reaching dimensions of 6,400×800. In addition, our DocPedia currently lacks the capability to process multi-page document images [44] and also exhibits a deficiency in multilingual proficiency [4].

## 6. Conclusion

This work introduces DocPedia, an innovative Large Multimodal Model tailored for versatile OCR-free document understanding, capable of handling images with high resolutions. Unlike existing methods, DocPedia directly processes visual input in the frequency domain, where more visual and textual information is captured in a limited number of visual tokens. Thanks to the dual-stage training strategy designed and the polished instructions/annotations for all tasks, DocPedia shows superior performance on several public datasets. In conclusion, we provide a successful attempt at pathways for handling complex high-resolution documents. We expect our success in exploring LMM dealing with high-resolution images from frequency perspective could trigger more insights for the community.

## References

- [1] Nasir Ahmed, T. Natarajan, and Kamisetty R Rao. Discrete cosine transform. *IEEE Transactions on Computers*, 100(1): 90–93, 1974. **2, 4**
- [2] Srikar Appalaraju, Bhavan Jasani, Bhargava Urala Kota, Yusheng Xie, and R Manmatha. DocFormer: End-to-end transformer for document understanding. In *ICCV*, pages 993–1003, 2021. **1, 3**
- [3] Haoli Bai, Zhiguang Liu, Xiaojun Meng, Wentao Li, Shuang Liu, Nian Xie, Rongfu Zheng, Liangwei Wang, Lu Hou, Jiansheng Wei, et al. Wukong-Reader: Multi-modal pre-training for fine-grained visual document understanding. *arXiv preprint arXiv:2212.09621*, 2022. **1, 3**
- [4] Jinze Bai, Shuai Bai, Shusheng Yang, Shijie Wang, Sinan Tan, Peng Wang, Junyang Lin, Chang Zhou, and Jingren Zhou. Qwen-VL: A frontier large vision-language model with versatile abilities. *arXiv preprint arXiv:2308.12966*, 2023. **8**
- [5] Ali Furkan Biten, Ruben Tito, Andres Mafla, Lluís Gomez, Marçal Rusinol, Minesh Mathew, CV Jawahar, Ernest Valveny, and Dimosthenis Karatzas. ICDAR 2019 competition on scene text visual question answering. In *ICDAR*, pages 1563–1570, 2019. **6**
- [6] Tom Brown, Benjamin Mann, Nick Ryder, Melanie Subbiah, Jared D Kaplan, Prafulla Dhariwal, Arvind Neelakantan, Pranav Shyam, Girish Sastry, Amanda Askell, et al. Language models are few-shot learners. *NeurIPS*, 33:1877–1901, 2020. **2, 5**
- [7] Wei-Lin Chiang, Zhuohan Li, Zi Lin, Ying Sheng, Zhanghao Wu, Hao Zhang, Lianmin Zheng, Siyuan Zhuang, Yonghao Zhuang, Joseph E Gonzalez, et al. Vicuna: An open-source chatbot impressing GPT-4 with 90%\* ChatGPT quality. See <https://vicuna.lmsys.org>, 2023. **2, 4, 5, 8**
- [8] Jacob Devlin, Ming-Wei Chang, Kenton Lee, and Kristina Toutanova. BERT: Pre-training of deep bidirectional transformers for language understanding. *arXiv preprint arXiv:1810.04805*, 2018. **3**
- [9] Hao Feng, Zijian Wang, Jingqun Tang, Jinghui Lu, Wengang Zhou, Houqiang Li, and Can Huang. UniDoc: A universal large multimodal model for simultaneous text detection, recognition, spotting and understanding. *arXiv preprint arXiv:2308.11592*, 2023. **1, 2, 3, 5, 6**
- [10] Kaiming He, Xinlei Chen, Saining Xie, Yanghao Li, Piotr Dollár, and Ross Girshick. Masked autoencoders are scalable vision learners. In *CVPR*, pages 16000–16009, 2022. **3**
- [11] Teakgyu Hong, Donghyun Kim, Mingi Ji, Wonseok Hwang, Daehyun Nam, and Sungrae Park. Bros: A pre-trained language model focusing on text and layout for better key information extraction from documents. In *AAAI*, pages 10767–10775, 2022. **1**
- [12] MD Zakir Hossain, Ferdous Sohel, Mohd Fairuz Shiratuddin, and Hamid Laga. A comprehensive survey of deep learning for image captioning. *ACM Computing Surveys*, 51(6): 1–36, 2019. **2, 4**
- [13] Yupan Huang, Tengchao Lv, Lei Cui, Yutong Lu, and Furu Wei. LayoutLMv3: Pre-training for document ai with unified text and image masking. In *ACM MM*, pages 4083–4091, 2022. **1, 3**
- [14] Zheng Huang, Kai Chen, Jianhua He, Xiang Bai, Dimosthenis Karatzas, Shijian Lu, and CV Jawahar. ICDAR 2019 competition on scanned receipt OCR and information extraction. In *ICDAR*, pages 1516–1520, 2019. **6**
- [15] Wonseok Hwang, Seonghyeon Kim, Minjoon Seo, Jinyeong Yim, Seunghyun Park, Sungrae Park, Junyeop Lee, Bado Lee, and Hwalsuk Lee. Post-OCR parsing: building simple and robust parser via bio tagging. In *NeurIPS*, 2019. **1**
- [16] Guillaume Jaume, Hazim Kemal Ekenel, and Jean-Philippe Thiran. Funsd: A dataset for form understanding in noisy scanned documents. In *ICDARW*, pages 1–6, 2019. **6**
- [17] Samira Ebrahimi Kahou, Vincent Michalski, Adam Atkinson, Ákos Kádár, Adam Trischler, and Yoshua Bengio. FigureQA: An annotated figure dataset for visual reasoning. *arXiv preprint arXiv:1710.07300*, 2017. **5**
- [18] Geewook Kim, Teakgyu Hong, Moonbin Yim, Jeongyeon Nam, Jinyoung Park, Jinyeong Yim, Wonseok Hwang, Sangdoo Yun, Dongyoon Han, and Seunghyun Park. OCR-free document understanding transformer. In *ECCV*, pages 498–517, 2022. **1, 2, 3, 4**
- [19] Jianfeng Kuang, Wei Hua, Dingkan Liang, Mingkun Yang, Deqiang Jiang, Bo Ren, and Xiang Bai. Visual information extraction in the wild: practical dataset and end-to-end solution. In *ICDAR*, pages 36–53, 2023. **6**
- [20] Kenton Lee, Mandar Joshi, Iulia Raluca Turc, Hexiang Hu, Fangyu Liu, Julian Martin Eisenschlos, Urvashi Khandelwal, Peter Shaw, Ming-Wei Chang, and Kristina Toutanova. Pix2Struct: Screenshot parsing as pretraining for visual language understanding. In *ICML*, pages 18893–18912, 2023. **2, 3**
- [21] Yulin Li, Yuxi Qian, Yuechen Yu, Xiameng Qin, Chengquan Zhang, Yan Liu, Kun Yao, Junyu Han, Jingtuo Liu, and Errui Ding. StrucTexT: Structured text understanding with multi-modal transformers. In *ACM MM*, pages 1912–1920, 2021. **1, 3**
- [22] Minghui Liao, Zhaoyi Wan, Cong Yao, Kai Chen, and Xiang Bai. Real-time scene text detection with differentiable binarization. In *AAAI*, pages 11474–11481, 2020. **1, 2, 4**
- [23] Hao Liu, Xinghua Jiang, Xin Li, Zhimin Bao, Deqiang Jiang, and Bo Ren. NomMer: Nominate synergistic context in vision transformer for visual recognition. In *CVPR*, pages 12073–12082, 2022. **2**
- [24] Hao Liu, Xinghua Jiang, Xin Li, Antai Guo, Yiqing Hu, Deqiang Jiang, and Bo Ren. The devil is in the frequency: Geminated gestalt autoencoder for self-supervised visual pre-training. In *AAAI*, pages 1649–1656, 2023. **2**
- [25] Haotian Liu, Chunyuan Li, Qingyang Wu, and Yong Jae Lee. Visual instruction tuning. *arXiv preprint arXiv:2304.08485*, 2023. **3, 4, 5, 6**
- [26] Xuebo Liu, Ding Liang, Shi Yan, Dagui Chen, Yu Qiao, and Junjie Yan. Fots: Fast oriented text spotting with a unified network. In *CVPR*, pages 5676–5685, 2018. **2, 4**
- [27] Yuliang Liu, Zhang Li, Hongliang Li, Wenwen Yu, Mingxin Huang, Dezhi Peng, Mingyu Liu, Mingrui Chen, Chunyuan Li, Lianwen Jin, et al. On the hidden mystery of OCR in

- large multimodal models. *arXiv preprint arXiv:2305.07895*, 2023. [2](#), [5](#), [6](#)
- [28] Ze Liu, Yutong Lin, Yue Cao, Han Hu, Yixuan Wei, Zheng Zhang, Stephen Lin, and Baining Guo. Swin transformer: Hierarchical vision transformer using shifted windows. In *ICCV*, pages 10012–10022, 2021. [4](#), [6](#)
- [29] Ilya Loshchilov and Frank Hutter. Decoupled weight decay regularization. *arXiv preprint arXiv:1711.05101*, 2017. [5](#)
- [30] Chuwei Luo, Changxu Cheng, Qi Zheng, and Cong Yao. GeoLayoutLM: Geometric pre-training for visual information extraction. In *CVPR*, pages 7092–7101, 2023. [1](#)
- [31] Tengchao Lv, Yupan Huang, Jingye Chen, Lei Cui, Shuming Ma, Yaoyao Chang, Shaohan Huang, Wenhui Wang, Li Dong, Weiyao Luo, et al. KOSMOS-2.5: A multimodal literate model. *arXiv preprint arXiv:2309.11419*, 2023. [1](#), [2](#), [3](#)
- [32] Ahmed Masry, Do Xuan Long, Jia Qing Tan, Shafiq Joty, and Enamul Hoque. ChartQA: A benchmark for question answering about charts with visual and logical reasoning. *arXiv preprint arXiv:2203.10244*, 2022. [5](#), [6](#)
- [33] Minesh Mathew, Dimosthenis Karatzas, and CV Jawahar. DocVQA: A dataset for VQA on document images. In *WACV*, pages 2200–2209, 2021. [4](#), [5](#), [6](#), [8](#)
- [34] Minesh Mathew, Viraj Bagal, Rubèn Tito, Dimosthenis Karatzas, Ernest Valveny, and CV Jawahar. InfographicVQA. In *WACV*, pages 1697–1706, 2022. [5](#), [6](#), [8](#)
- [35] Anand Mishra, Shashank Shekhar, Ajeet Kumar Singh, and Anirban Chakraborty. OCR-VQA: Visual question answering by reading text in images. In *ICDAR*, pages 947–952, 2019. [5](#), [6](#)
- [36] Qiming Peng, Yinxu Pan, Wenjin Wang, Bin Luo, Zhenyu Zhang, Zhengjie Huang, Teng Hu, Weichong Yin, Yongfeng Chen, Yin Zhang, et al. Ernie-layout: Layout knowledge enhanced pre-training for visually-rich document understanding. *arXiv preprint arXiv:2210.06155*, 2022. [1](#)
- [37] Zhiliang Peng, Wenhui Wang, Li Dong, Yaru Hao, Shaohan Huang, Shuming Ma, and Furu Wei. KOSMOS-2: Grounding multimodal large language models to the world. *arXiv preprint arXiv:2306.14824*, 2023. [3](#)
- [38] Alec Radford, Jong Wook Kim, Chris Hallacy, Aditya Ramesh, Gabriel Goh, Sandhini Agarwal, Girish Sastry, Amanda Askell, Pamela Mishkin, Jack Clark, et al. Learning transferable visual models from natural language supervision. In *ICML*, pages 8748–8763, 2021. [2](#), [3](#), [6](#)
- [39] Baoguang Shi, Xiang Bai, and Cong Yao. An end-to-end trainable neural network for image-based sequence recognition and its application to scene text recognition. *TPAMI*, 39(11):2298–2304, 2016. [1](#)
- [40] Amanpreet Singh, Vivek Natarajan, Meet Shah, Yu Jiang, Xinlei Chen, Dhruv Batra, Devi Parikh, and Marcus Rohrbach. Towards VQA models that can read. In *CVPR*, pages 8317–8326, 2019. [5](#), [6](#), [8](#)
- [41] Leslie N Smith and Nicholay Topin. Super-convergence: Very fast training of neural networks using large learning rates. In *AIMLMOA*, pages 369–386, 2019. [5](#)
- [42] Sargur N Srihari, Stephen W Lam, Venu Govindaraju, R Srihari, and Jonathan J Hull. Document image understanding. In *FJCC*, pages 87–95, 1986. [1](#)
- [43] Zineng Tang, Ziyi Yang, Guoxin Wang, Yuwei Fang, Yang Liu, Chenguang Zhu, Michael Zeng, Cha Zhang, and Mohit Bansal. Unifying vision, text, and layout for universal document processing. In *CVPR*, pages 19254–19264, 2023. [1](#)
- [44] Rubèn Tito, Dimosthenis Karatzas, and Ernest Valveny. Hierarchical multimodal transformers for multipage DocVQA. *PR*, 144:109834, 2023. [8](#)
- [45] Hugo Touvron, Thibaut Lavril, Gautier Izacard, Xavier Martinet, Marie-Anne Lachaux, Timothée Lacroix, Baptiste Rozière, Naman Goyal, Eric Hambro, Faisal Azhar, et al. LLaMA: Open and efficient foundation language models. *arXiv preprint arXiv:2302.13971*, 2023. [2](#)
- [46] Ashish Vaswani, Noam Shazeer, Niki Parmar, Jakob Uszkoreit, Llion Jones, Aidan N Gomez, Łukasz Kaiser, and Illia Polosukhin. Attention is all you need. *NeurIPS*, 30, 2017. [2](#)
- [47] Gregory K Wallace. The jpeg still picture compression standard. *Commun. ACM*, 34(4):30–44, 1991. [2](#), [4](#)
- [48] Kai Wang, Boris Babenko, and Serge Belongie. End-to-end scene text recognition. In *ICCV*, pages 1457–1464, 2011. [4](#)
- [49] Yiheng Xu, Minghao Li, Lei Cui, Shaohan Huang, Furu Wei, and Ming Zhou. LayoutLM: Pre-training of text and layout for document image understanding. In *KDD*, pages 1192–1200, 2020. [1](#), [3](#)
- [50] Yiheng Xu, Tengchao Lv, Lei Cui, Guoxin Wang, Yijuan Lu, Dinei Florencio, Cha Zhang, and Furu Wei. LayoutLM: Multimodal pre-training for multilingual visually-rich document understanding. *arXiv preprint arXiv:2104.08836*, 2021. [1](#), [3](#)
- [51] Jiabo Ye, Anwen Hu, Haiyang Xu, Qinghao Ye, Ming Yan, Yuhao Dan, Chenlin Zhao, Guohai Xu, Chenliang Li, Junfeng Tian, et al. mPLUG-DocOwl: Modularized multimodal large language model for document understanding. *arXiv preprint arXiv:2307.02499*, 2023. [2](#), [3](#)
- [52] Jiabo Ye, Anwen Hu, Haiyang Xu, Qinghao Ye, Ming Yan, Guohai Xu, Chenliang Li, Junfeng Tian, Qi Qian, Ji Zhang, et al. UReader: Universal OCR-free visually-situated language understanding with multimodal large language model. *arXiv preprint arXiv:2310.05126*, 2023. [1](#), [2](#), [3](#)
- [53] Qinghao Ye, Haiyang Xu, Guohai Xu, Jiabo Ye, Ming Yan, Yiyang Zhou, Junyang Wang, Anwen Hu, Pengcheng Shi, Yaya Shi, et al. mPLUG-Owl: Modularization empowers large language models with multimodality. *arXiv preprint arXiv:2304.14178*, 2023. [1](#), [2](#), [3](#)
- [54] Yuechen Yu, Yulin Li, Chengquan Zhang, Xiaoqiang Zhang, Zengyuan Guo, Xiameng Qin, Kun Yao, Junyu Han, Errui Ding, and Jingdong Wang. StrucTexTv2: Masked visual-textual prediction for document image pre-training. *arXiv preprint arXiv:2303.00289*, 2023. [3](#)
- [55] Yanzhe Zhang, Ruiyi Zhang, Jiuxiang Gu, Yufan Zhou, Nedim Lipka, Diyi Yang, and Tong Sun. LLaVAR: Enhanced visual instruction tuning for text-rich image understanding. *arXiv preprint arXiv:2306.17107*, 2023. [2](#), [3](#)
- [56] Deyao Zhu, Jun Chen, Xiaoqian Shen, Xiang Li, and Mohamed Elhoseiny. MiniGPT-4: Enhancing vision-language understanding with advanced large language models. *arXiv preprint arXiv:2304.10592*, 2023. [4](#), [6](#)

# DocPedia: Unleashing the Power of Large Multimodal Model in the Frequency Domain for Versatile Document Understanding (Supplementary Material)

Hao Feng<sup>1,2,♠,\*</sup> Qi Liu<sup>2,\*</sup>, Hao Liu<sup>2,\*</sup>,<sup>‡</sup> Wengang Zhou<sup>1,‡</sup> Houqiang Li<sup>1</sup> Can Huang<sup>2,‡</sup>

<sup>1</sup> University of Science and Technology of China, <sup>2</sup> ByteDance Inc.,

{haof}@mail.ustc.edu.cn, {zhwg, lihq}@ustc.edu.cn,

{liuqi.nero, haoliu.0128, can.huang}@bytedance.com

*This supplementary material includes some implementation details that are not included in the main text of the manuscript due to space constraints.*

## A. Preliminary: Discrete Cosine Transform

In this discussion, we elucidate the extraction process of Discrete Cosine Transform (DCT) coefficients [1], which is fundamental for the design of our DocPedia. The extraction process unfolds as follows:

- An  $H \times W \times 3$  RGB image is taken as input.
- It is then transformed to YCbCr color space.
- The Cb and Cr channels undergo subsampling, reducing their dimensions to  $\frac{H}{2} \times \frac{W}{2}$ .
- The pixel value range is adjusted from [0,255] to [-128,127], centering it around zero.
- Subsequently, the DCT is applied to  $8 \times 8$  non-overlapping pixel blocks.
- Finally, the DCT coefficients are quantized.

Among them, the Discrete Cosine Transform is a technique that breaks down a finite sequence of data into a summation of cosine functions with discrete frequencies. This transformation shifts the data from the spatial domain to the frequency domain. Our focus is on the  $8 \times 8$  DCT, a cornerstone of JPEG encoding. Consider  $\mathbf{x} \in \mathbb{R}^{8 \times 8}$  as an image patch of dimension  $8 \times 8$ . The DCT of  $\mathbf{x}$ , denoted as  $\mathbf{X} \in \mathbb{R}^{8 \times 8}$ , is computed as follows:

$$\mathbf{X}_{u,v} = \frac{\alpha_u \alpha_v}{4} \sum_{m,n} \mathbf{x}_{m,n} \cos \left[ \frac{\pi(2m+1)u}{16} \right] \cos \left[ \frac{\pi(2n+1)v}{16} \right]. \quad (1)$$

where  $\alpha_i$  is assigned a value of  $1/\sqrt{2}$  if  $i = 0$ , otherwise it is 1. The indices  $u, v, m, n$  are within the range [0, 7].

\*Equal contribution. ♠ Interns at ByteDance. ‡ Project lead.

†Corresponding authors: Wengang Zhou and Can Huang.

No.	Instructions
1	Extract all the text in <term>.
2	Can you identify the words in <term>?
3	Tell me the text you see in <term>.
4	What’s written in <term>?
5	Decode the text from <term>.
6	Reveal the text in <term> for me.
7	Detail the text present in <term>.
8	Elaborate on the words in <term>.
9	Illuminate me with the text from <term>.
10	Narrate the words you find in <term>.
11	Can you spell out the text from <term>?
12	I’d like to know the words in <term>.
13	Dissect <term> and tell me its text.
14	I’m curious about the text in <term>. What is it?
15	Help me decipher the words in <term>.
16	Shed light on the text of <term>.
17	Convey the written part of <term> to me.
18	Identify the text in <term>.
19	What’s the text in <term>.
20	Recognize all the text in <term>.

Table A1. Instruction templates for the **text recognition** task. The <term> placeholder denotes strings formed by a random determiner and an image noun, such as “this image” or “the photo”, etc., to enhance the variability of the instructions.

This formulation encapsulates the essence of transforming an image patch into its frequency domain representation.

## B. Instruction Templates

During the pre-training and fine-tuning stage, we train our DocPedia on five text-aware tasks to enhance the perception ability on the text content in the image. For each image, we randomly select one of these tasks to create the instruction and corresponding ground truth response. Here we present the instructional templates of these five tasks, including text

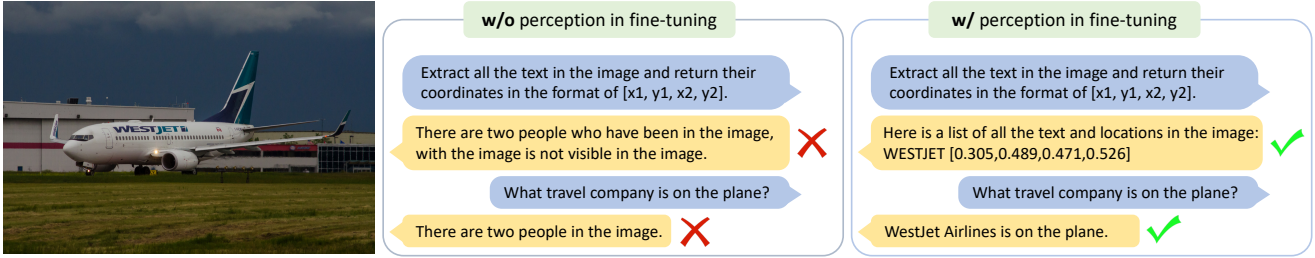


Figure A1. Illustration demonstrating the impact of **joint learning of perception and comprehension** during the fine-tuning phase. We present a comparison between two models under the same conditions: a given image with identical spotting and understanding instructions. The model fine-tuned solely on the understanding task (middle) responds incorrectly to both instructions, whereas the model undergoing joint learning of perception and understanding tasks (right) during fine-tuning phase answers both tasks correctly.

No.	Instructions
1	Output all the text’s locations in <term>.
2	Where are the texts located in <term>?
3	Locate the texts in <term> for me.
4	Highlight the positions of all the texts in <term>.
5	I need the coordinates of the texts in <term>.
6	Show me the regions with texts in <term>.
7	Determine the areas with text in <term>.
8	Can you pinpoint the text locations in <term>?
9	Map out the texts in <term> for me.
10	Display the text positions in <term>.

Table B2. Instruction templates for the **text detection** task. The <term> placeholder denotes strings formed by a random determiner and an image noun, such as “this image” or “the photo”, etc., to enhance the variability of the instructions.

No.	Instructions
1	Give a detailed reading of <term>.
2	Can you provide a full reading from <term>.
3	Read aloud the text from <term>.
4	Convey the entire content of <term> to me.
5	I’d like a comprehensive reading of <term>.
6	Recite the content from <term> for me.
7	Provide a transcript of the text from <term>.
8	I want to hear the text from <term>.
9	Narrate the entire text of <term> for me.
10	Please read out the full text from <term>.

Table B3. Instruction templates for the **full-text reading** task. The <term> placeholder denotes strings formed by a random determiner and an image noun, such as “this image” or “the photo”, etc., to enhance the variability of the instructions.

recognition in Table A1, text detection in Table B2, text spotting in Table B5, paragraph reading in Table B6, and full-text reading in Table B3. These templates are generated using GPT 3.5 [2] to expand their diversity.

Method		VQA		
Input	Resolution	Tokens	DocVQA [4]	TextVQA [5]
RGB Flattening	1920×1920	900	30.44	46.34
DCT	1920×1920	900	<b>37.83</b>	<b>53.35</b>
RGB Flattening	2560×2560	1600	39.25	51.63
DCT	2560×2560	1600	<b>47.08</b>	<b>60.18</b>

Table B4. Comparative experiments about the necessity of DCT.

## C. Further Analysis on DocPedia

**Perception facilitates comprehension.** By default, we perform joint learning of perception and comprehension tasks during the fine-tuning phase. We argue that employing such a fine-tuning strategy compels the model to visually perceive the informative cues prior to comprehending the content, which has been verified in Table 5 of the main text. Moreover, we provide a vivid example in Fig. A1 to confirm the facilitation of perception to comprehension. Concretely, we compare the responses of two models under identical conditions: the same image and instructions for spotting and understanding. The model (“w/o perception in fine-tuning”), which is fine-tuned merely with the understanding task (middle), fails to recognize the target text on the plane and responds the problematic answer to the understanding question. In contrast, the other model (“w/ perception in fine-tuning”) fine-tuned on both perception and understanding tasks, accurately responds to the two instructions.

**Indispensable DCT.** To further investigate the necessity of frequency learning in enhancing input image resolution, we conducted comparative experiments involving different input processing techniques (RGB Flattening vs. DCT), as outlined in Table B4. Specifically, in the “RGB Flattening” approach, we initially divided the input image ( $H \times W \times 3$ ) into non-overlapping patches of size  $8 \times 8 \times 3$  without applying the DCT. Subsequently, each patch was directly unfolded into a  $1 \times 1 \times 192$  vector, forming a resulting cube



Do you know which company created this game?

Yes, I can confirm that Super Mario Bros was created by Nintendo.



Who sold this ticket?

The person who sold this ticket is Maarten.



Where is Tesla's headquarters according to the image?

According to the image, the headquarters of Tesla is located in Austin, Texas.



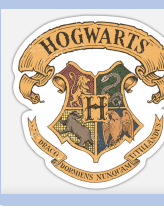
Who wrote this letter?

The person who wrote this letter is Jeffrey Hammond.



Where is the valet parking?

The valet parking is located at B2.



Which novel does this badge belong to and why?

This badge is associated with the Hogwarts School of Witchcraft and Magic in the Harry Potter series of novels. It represents the school emblem and serves as a symbol of pride for graduates or students attending the school.



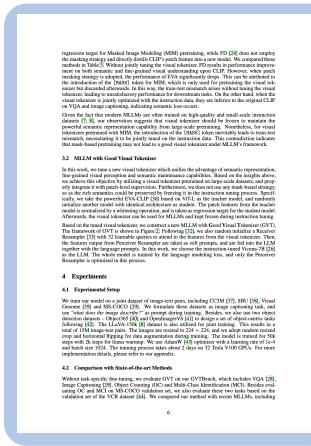
What is the transportation tool should I choose if I want to browse around the Amsterdam?

If you want to browse around Amsterdam, one of the best transportation tools is bicycles.



What is the name of the station in this image?

The name of the station is Den Haag Central.



What does GVT stand for according to the paper?

According to the paper, GVT stands for Good Visual Tokenizer.

Figure B2. Exemplary demonstrations of DocPedia’s image comprehension capabilities. DocPedia accurately responds to instructions by analyzing both visual and textual information within images. It demonstrates effective proficiency in interpreting scene text images and document images. Notably, it exhibits robust performance in processing images containing text of varying sizes, fonts, and styles.

No.	Instructions
1	Recognize all the text in <term> and return their positions [x1, y1, x2, y2].
2	Extract all the text in <term> and return their coordinates in the format of [x1, y1, x2, y2].
3	Identify the text in <term> and return their [x1, y1, x2, y2] coordinates.
4	Identify the text in <term> and return their positions in the format of [x1, y1, x2, y2].
5	Recognize all the text in <term> return their coordinates in the format of [x1, y1, x2, y2].
6	Detect the text in <term> and return their coordinates in the format of [x1, y1, x2, y2].
7	Find all the text in <term> and return their coordinates in the format of [x1, y1, x2, y2].
8	Find all the text in <term> and return their positions represented in the format of [x1, y1, x2, y2].
9	Parse all the text in <term> and return their coordinates in the format of [x1, y1, x2, y2].
10	Interpret all text in <term> and output their coordinates in the format [x1, y1, x2, y2].

Table B5. Instruction templates for the **text spotting** task. The <term> placeholder denotes strings formed by a random determiner and an image noun, such as “this image” or “the photo”, etc., to enhance the variability of the instructions.

No.	Instructions
1	What text is inside the region <box> in <term>?
2	Tell me about the content in the area marked as <box> of <term>.
3	I’m curious about the text in the section denoted by <box> of <term>.
4	What does <term> say in the area outlined by <box>?
5	Decipher the words within the space defined by <box> in <term>.
6	Can you read the text from the section specified as <box> in <term>.
7	Reveal the content of the region marked as <box> in <term>.
8	Extract the words from the portion designated by <box> in <term>.
9	I’d like to know the text from the highlighted box given by <box> in <term>.
10	Decode the inscription inside the region defined by <box> in <term>.

Table B6. Instruction templates for the **paragraph reading** task. The <term> placeholder denotes strings formed by a random determiner and an image noun, such as “this image” or “the photo”, etc. The <box> represents a bounding box string that indicates a text paragraph.

of size  $\frac{H}{8} \times \frac{W}{8} \times 192$ , which shares a similar shape with the counterpart in our “DCT” approach.

From the observations presented in Table B4, it is evident that employing the “DCT” method consistently yields significantly higher performance, whether with a resolution of 1,920 or 2,560, compared to the simplistic “RGB Flattening” technique. Moreover, we surprisingly find that introducing DCT leads to more stable and faster convergence during training, particularly when dealing with high-resolution document images. We attribute these phenomena to the unique characteristics of DCT. As an orthogonal transformation, DCT decouples and orthogonalizes frequency components, effectively reducing input redundancy. In contrast, direct flattening in the RGB space lacks this capability. Although it can be partially compensated for through learning from large-scale data using convolutional or linear layers [3], it is evident that they do not achieve the same level of direct redundancy reduction as the DCT.

## D. More Qualitative Results

We further present more qualitative results of our DocPedia to exhibit its comprehension capacities. As shown in Fig. B2, our DocPedia is capable of extracting pertinent visual and textual information from high-resolution scene text

images and document images in response to instructions, thereby enabling it to provide accurate answers. This reveals the superiority of our method. Moreover, it is evident that our DocPedia exhibits strong generalization capabilities in handling images containing text with various style, size, and font. This proficiency is attributed to our extensive instruction-following dataset, covering scene text images and various forms of document images.

## References

- [1] Nasir Ahmed, T. Natarajan, and Kamisetty R Rao. Discrete cosine transform. *IEEE Transactions on Computers*, 100(1): 90–93, 1974. 1
- [2] Tom Brown, Benjamin Mann, Nick Ryder, Melanie Subbiah, Jared D Kaplan, Prafulla Dhariwal, Arvind Neelakantan, Pranav Shyam, Girish Sastry, Amanda Askell, et al. Language models are few-shot learners. *NeurIPS*, 33:1877–1901, 2020. 2
- [3] Alexey Dosovitskiy, Lucas Beyer, Alexander Kolesnikov, Dirk Weissenborn, Xiaohua Zhai, Thomas Unterthiner, Mostafa Dehghani, Matthias Minderer, Georg Heigold, Sylvain Gelly, et al. An image is worth 16x16 words: Transformers for image recognition at scale. *arXiv preprint arXiv:2010.11929*, 2020. 4
- [4] Minesh Mathew, Dimosthenis Karatzas, and CV Jawahar.

DocVQA: A dataset for VQA on document images. In *WACV*, pages 2200–2209, 2021. [2](#)

- [5] Amanpreet Singh, Vivek Natarajan, Meet Shah, Yu Jiang, Xinlei Chen, Dhruv Batra, Devi Parikh, and Marcus Rohrbach. Towards VQA models that can read. In *CVPR*, pages 8317–8326, 2019. [2](#)